Food Chemistry 443 (2024) 138504

Contents lists available at ScienceDirect

Food Chemistry

journal homepage: www.elsevier.com/locate/foodchem

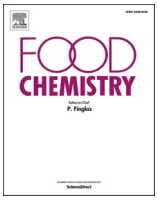

From waste to bioactive compounds: A response surface methodology approach to extract antioxidants from *Pistacia vera* shells for postprandial hyperglycaemia management

Anna Elisabetta Maccarronello [a], Nunzio Cardullo [a], Ana Margarida Silva [b], Antonella Di Francesco [a], Paulo C. Costa [c,d], Francisca Rodrigues [b,*], Vera Muccilli [a,*]

[a] *University of Catania, Department of Chemical Sciences, Viale A. Doria 6, 95125 Catania, Italy*
[b] *REQUIMTE/LAQV, ISEP, Polytechnic of Porto, Rua Dr. António Bernardino de Almeida, 4249-015 Porto, Portugal*
[c] *UCIBIO, Applied Molecular Biosciences Unit, MedTech-Laboratory of Pharmaceutical Technology, Faculty of Pharmacy, University of Porto, Rua de Jorge Viterbo Ferreira, 228, 4050-313 Porto, Portugal*
[d] *Associate Laboratory i4HB - Institute for Health and Bioeconomy, Faculty of Pharmacy, University of Porto, 4050-313 Porto, Portugal*

A R T I C L E I N F O

Keywords:
Microwave-assisted extraction
Response surface methodology
HPLC-MS
Antioxidant
α-glucosidase inhibition
α-amylase inhibition

A B S T R A C T

Pistacia vera shells, an abundant agricultural by-product, are a rich source of undiscovered bioactive compounds. This study employed a response surface methodology (RSM) approach to optimize the microwave-assisted extraction of antioxidants. The highest total phenolic content, and antioxidant activity were achieved under the optimized extraction conditions (20 % ethanol, 1000 W, 135 s, and solvent-to-solid ratio of 27 mL/g). The resulting extract (OPVS-E) included gallic acid derivatives, hydrolysable tannins, flavonoids, fatty acids, and anacardic acids. Remarkably, OPVS-E displayed potent inhibitory activity against α-amylase (IC_{50} = 2.05 μg/mL) and α-glucosidase (IC_{50} = 41.07 μg/mL), by far more powerful than the anti-diabetic drug acarbose, OPVS-E exhibited a strong antiradical capacity against reactive oxygen species (ROS) without causing toxicity in intestinal cells (HT29-MTX and Caco-2). These findings introduce OPVS-E as a potential novel dual-action nutraceutical ingredient, able to mitigate postprandial hyperglycemia and counteract the ROS overproduction occurring in type 2 diabetes mellitus.

1. Introduction

In the last decades, polyphenols have been the subject of extensive research aimed at deepening the understanding of their potential health benefits and exploring their therapeutic applications in the prevention and management of chronic diseases, providing scientific evidence for their inclusion in nutraceutical formulations (Pinto, Vieira, et al., 2021). It is well-stated that polyphenols can effectively neutralize the reactive oxygen and nitrogen species (ROS, RNS) produced by the human body, avoiding the propagation of free radical chains, and acting as exogenous antioxidants (Nayak et al., 2015; Pandey & Rizvi, 2009). Recently, a correlation between excessive ROS production and type 2 diabetes mellitus (T2DM) has been demonstrated. ROS overproduction contributes to pancreatic β-cell dysfunction, insulin resistance, and T2DM cardiovascular complications (Fiorentino, Prioletta, Zuo, & Folli, 2013; Ullah, Khan, & Khan, 2016). One of the current therapeutic approaches to counteract postprandial hyperglycemia aims to slow down the carbohydrate intestinal absorption by administrating α-amylase and α-glucosidase inhibitors, such as acarbose or miglitol (Kumar & Sinha, 2012). Nevertheless, the intake of these drugs is accompanied by various adverse effects, such as gastrointestinal issues and skin reactions (Kumar & Sinha, 2012), prompting ongoing research for novel natural alternatives (Tundis, Loizzo, & Menichini, 2010) characterised by negligible side effects.

Pistacia vera L. is a plant tree widely cultivated in Iran, the United States of America (USA), and Turkey (Toghiani, Fallah, Nasernejad, Mahboubi, Taherzadeh, & Afsham, 2023), whose edible nuts, commonly known as pistachios, are worldwide appreciated for their distinctive taste and nutritional benefits (Terzo et al., 2019). Pistachio global production accounted for over 900 kilotons in 2021 (FAOSTAT). Unavoidably, such production involves the generation of massive quantities of waste biomass, skins (seed coat), hulls (green shell cover),

* Corresponding authors.
E-mail addresses: francisca.rodrigues@graq.isep.ipp.pt (F. Rodrigues), vera.muccilli@unict.it (V. Muccilli).

https://doi.org/10.1016/j.foodchem.2024.138504
Received 20 October 2023; Received in revised form 15 January 2024; Accepted 17 January 2024
Available online 21 January 2024

and shells (lignified hardened endocarp). *Pistacia vera* shells (PVS) represent almost 70 % of the by-products generated and accumulated during industrial dehulling. Up to date, no utilization is reported for PVS being just employed as a low-value energy source (Toghiani et al., 2023) since lignin (13.5 %) and cellulose (42 %) account for the major constituents of this material (Yeganeh, Kaghazchi, & Soleimani, 2006). However, the pressing environmental challenges, particularly pollution and resource scarcity, along with a concurrent major consumer's preference towards products derived from natural sources, resulted in a growing recognition of the waste biomasses' ecological and economic value. The recovery of polyphenols from agri-food industrial by-products has attracted much attention due to their plethora of health-promoting properties (Pandey et al., 2009). Recently, PVS have been reported as a source of phenolic compounds that can be extracted with different extraction methods employing alcoholic solutions (Cardullo, Leanza, Muccilli, & Tringali, 2021). Nevertheless, optimizing an effective extraction procedure is a key step to promote the exploitation of PVS as a renewable source of phytochemicals. Among eco-friendly techniques, microwave-assisted extraction (MAE) emerged as a sustainable alternative to conventional methods such as maceration and hydrodistillation. In fact, MAE is characterized by a low environmental and economic impact, employing low solvent quantities, short extraction times, and leading to high-quality extracts with less energy consumption (Alvi, Asif, & Khan, 2022). Moreover, MAE can be employed with generally recognised as safe solvents (GRAS), such as ethanol. Despite the outstanding characteristics offered by MAE, some extraction parameters must be carefully considered, including the solvent concentration, the irradiation time, the microwave (MW) power, and solvent-to-solid ratio (Nayak et al., 2015). To find the best MAE operating conditions and, consequently, maximize the recovery of bioactive compounds, mathematical tools such as the response surface methodology (RSM) can be effectively employed (Weremfo, Abassah-Oppong, Adulley, Dabie, & Seidu-Larry, 2023). RSM allows a deeper understanding of the system under study by providing insights into the relationship between multiple independent variables, or factors, and the dependent variables, or responses. Furthermore, RSM reduces the number of required experiments compared to the traditional one-factor-at-a-time approach, saving time and resources (Bonaccorso et al., 2021). RSM has already been adopted for the optimization of polyphenols extraction from various plant-based foods and their by-products (Pinto et al., 2020; Pinto, Vieira, et al., 2021; Silva, Pinto, Moreira, Costa, Delerue-Matos, & Rodrigues, 2022). Therefore, this study aimed to optimize a MAE protocol by RSM to maximize the recovery of polyphenols and antioxidant/antiradical compounds from PVS, determining the potential anti-diabetic action of the optimized extract (OPVS-E) in maintaining the glucose homeostasis and counteracting the ROS overproduction that occurs in T2DM.

2. Materials and methods

2.1. Pistacia vera shells

PVS were kindly supplied by a local pistachio manufacturer from Bronte (Catania, Italy) in December 2021. Shells were washed three times with distilled water to remove other residues, such as branches and green hulls, and dried in a forced oven at 35 °C. Afterwards, shells were ground using an electrical grinder (KYG model-CG9430, 300 W) and passed through a 1 mm sieve to ensure homogeneity, being stored at room temperature (20 °C) and protected from light until extractions.

2.2. Chemicals

All chemicals were of analytical (or superior) grade, used as received from commercial sources. HPLC grade standards (17:1) anacardic acid and quercetin-3-*O*-glucoside were purchased from Thermo Fisher (Kandel, Germany). Acetonitrile, formic acid (FA), methanol (MeOH), 96 % ethanol (EtOH), Folin-Ciocalteau's reagent, 1,1-diphenyl-2-picrylhydrazyl free radical (DPPH•) and 2,4,6-tri(2-pyridyl)-1,3,5-triazine (TPTZ) were acquired from Merck (Darmstadt, Germany). Trolox (6-hydroxy-2,5,7,8-tetramethylchroman-2-carboxylic acid), potassium persulfate ($K_2S_2O_8$), 2,20-azino-bis(3-ethylbenzothiazoline-6-sulfonic acid) diammonium salt ($ABTS^{\bullet}$), nitro blue tetrazolium chloride (NBT), β-nicotinamide adenine dinucleotide (NADH), sodium hypochlorite solution with 4 % available chlorine, dihydrorhodamine 123 (DHR), phenazine methosulphate (PMS), α,α'-azodiisobutyramidine dihydrochloride (AAPH), and fluorescein sodium salt were purchased from Sigma Aldrich (Steinheim, Germany), whereas catechin, gallic acid, and Triton X-100 were purchased from Sigma Chemical Co. (St. Louis, USA). Dulbecco's Modified Eagle medium (DMEM), non-essential amino acids, and Hank's Balanced Salt Solution (HBSS) were purchased from Biowest SAS (Nuaillé, France). Fetal bovine serum (FBS) Supreme was obtained from PAN-Biotech (Aidenbach, Germany). TrypLE Express was obtained from Gibco (Life Technologies, S.A., Madrid, Spain). Dimethyl sulfoxide (DMSO) was purchased from AppliChem (Darmstadt, Germany). MilliQ-water was employed in all the experiments.

2.3. Microwave-assisted extraction (MAE)

Bioactive compounds from PVS were extracted with a domestic microwave oven (Smeg S43 Type F322EC, RE, Italy). The instrument was equipped with a digital control screen to set up the desired extraction time and the MW power (150 to 1000 W). The oven was modified with a hole on the top (18 mm diameter) and a chilled water system to condense the vapours generated during the extraction procedures. The homogenized PVS powder (100 mg) was mixed with the appropriate amount of solvent mixture and subjected to MAE. The sample temperature measured after each extraction never exceeded 64 °C. After MAE, the extracts were filtered through cotton, and the supernatant was collected and dried in a vacuum concentrator (Concentrator plus/Vacufuge® plus – Eppendorf, Hamburg, Germany). The dried extracts were stored at −10 °C until further analyses.

2.4. Experimental design for optimization of MAE conditions

RSM with a four-factorial Box-Behnken experimental design (BBD) was employed to evaluate the effects of operating extraction variables (X_1 – X_4) on the total phenolic content (TPC) and antioxidant activity (evaluated by FRAP, DPPH•, and $ABTS^{\bullet+}$ assays), thus providing the optimal extraction conditions to maximize the recovery of bioactive compounds from PVS.

EtOH percentage, MW power, irradiation time, and solvent-to-solid ratio were changed each time, according to the experimental design reported in Table 2. This latest was generated using the JMP® statistical software (SAS Institute S.r.l., Milano, Italy). A total of 27-runs of experiments were performed according to Equation (1):

$$N = 2k(k-1) + C_o \quad (1)$$

where k is the number of factors, and C_0 is the number of central points. Three levels coded as −1 (low), 0 (middle), and + 1 (high) were considered for each factor under study. All the extractions were randomly carried out to minimize the effect of unexplained variability in the measured responses caused by systematic errors. Afterward, the dependent variables, including TPC (Y_1), FRAP (Y_2), $DPPH^{\bullet}$ (Y_3), and $ABTS^{\bullet+}$ (Y_4), were fitted with a second-order quadratic model, according to Equation (2):

$$Y = B_0 + \sum_{i=1}^{k} B_i X_i + \sum_{i=1}^{k} B_{ii} X^2 + \sum_{i>j}^{k} B_{ij} X_i X_j + E \quad (2)$$

where Y represents the predicted response; X represents the independent variable; B_0 is the intercept; B_i, B_{ii}, and B_{ij} are the linear, quadratic, and

interactive regression coefficients, respectively (Nayak et al., 2015). The regression coefficients were determined based on the analysis of variance (ANOVA), where a p-value < 0.05 (Tukey's test) was considered statistically significant. Three-dimensional response surface plots were used as visual tools to analyse the interactions among factors and responses and deduce the optimal factor combinations to achieve the desired outcomes. Model adequacy was evaluated using the lack of fit, the coefficient of determination (R^2), and the F-test values. Following the optimal MAE conditions estimated by the model, the optimized extract from PVS (OPVS-E) was obtained in triplicate.

2.5. Determination of the total phenolic content (TPC)

The TPC of the PVS extracts obtained according to the RSM (Table 2) and that of the final optimized extract (OPVS-E) was spectrophotometrically determined in 96-well microplates using an Agilent BioTek Synergy H1 Multimode Reader and the Gen5 software, following the procedure described by Cardullo *et al.* (Cardullo, Leanza, et al., 2021). Sample solutions were prepared in a mixture of MeOH/H_2O (50:50, *v/v*) to a final concentration of 0.5 mg/mL. Different concentrations of gallic acid (0.05 – 0.5 mg/mL) were assayed in the same conditions to obtain a calibration curve ($R^2 = 0.9992$). The solutions were incubated at room temperature and in the dark for 1 h and 30 min. Then, optical density (OD) was read at 765 nm. Results were reported as mg of gallic acid equivalents per g of PVS dry weight (mg GAE/g DW). All measurements were carried out in quadruplicate and reported as mean ± SD.

2.6. In vitro studies: antioxidant/antiradical activities, α-glucosidase, and α-amylase inhibition

PVS extracts obtained according to the RSM design (Table 2), and the OPVS-E were subjected to *in vitro* antioxidant assays (FRAP, DPPH, and ABTS) as detailed below. α-Glucosidase and α-amylase inhibitory activity, as well as the radical scavenging capacity against ROS, were assayed only on the OPVS-E sample.

2.6.1. Ferric reducing antioxidant power (FRAP) assay

PVS extracts' capacity to reduce ferric ions was assessed using a previously reported method, with minor modifications (Ngoh & Gan, 2016). Briefly, a 10 mM TPTZ solution in 40 mM HCl, and a 20 mM $FeCI_3$ solution were mixed in acetate buffer (300 mM, pH 3.6) at 1:1:10 ratio to obtain the FRAP reagent. The resulting FRAP solution was incubated under stirring at 37 °C for 30 min, in the dark. Then, 20 μL of samples (0.5 mg/mL in 50:50 MeOH: H_2O) or quercetin (0.1 mg/mL) employed as a positive control, were mixed with FRAP solution (200 μL) into a 96-well microplate. Blank solutions were obtained, replacing the samples with the same volume of methanol. Additionally, a calibration curve ($R^2 = 0.9899$) was obtained from different concentrations (25 – 1000 μM) of Trolox. The microplate was incubated for 30 min at 37 °C in the darkness and the OD was read at 593 nm. Each sample was assayed in quadruplicate and the results were expressed as mg of TE (Trolox Equivalents) per gram of PVS dry weight (mg TE/g DW).

2.6.2. Scavenging capacity against the DPPH$^\bullet$

The electron donation ability of PVS extracts was measured through the bleaching of the purple-coloured DPPH$^\bullet$ solution, as previously described by Cardullo *et al.* (Cardullo, Leanza, et al., 2021). Briefly, a freshly prepared 190 μM DPPH$^\bullet$ solution was mixed with the tested samples (0.5 mg/mL; 20 μL). A blank was obtained replacing the tested samples with the same amount of methanol. Quercetin was used as positive control (0.05 mg/mL). Trolox (0.1 – 0.8 mM) was employed as a standard to achieve a calibration curve ($R^2 = 0.9974$). The mixtures were incubated at 25 °C for 1 h and 30 min in the dark. Then, OD was acquired at 515 nm and the antiradical activity of the extracts was determined as the percentage of inhibition of DPPH$^\bullet$ radical calculated according to Equation (3):

$$QuenchedDPPH(\%) = \frac{(OD_{blank} - OD_{sample})}{OD_{blank}} \times 100 \quad (3)$$

The results were expressed as μg of Trolox equivalents (TE) per gram of PVS dry weight (μg TE/g DW).

2.6.3. Scavenging capacity against the ABTS$^{\bullet+}$

The ability of the PVS extracts to scavenge ABTS$^{\bullet+}$ was investigated according to the method validated by Cardullo *et al.* (Cardullo, Leanza, et al., 2021). ABTS$^{\bullet+}$ was previously generated by mixing 7 mM of ABTS stock solution with 2.45 mM of potassium persulfate ($K_2S_2O_8$) and incubating for 16 h at room temperature in the dark. ABTS$^{\bullet+}$ was diluted in ethanol to a final concentration of 70 μM and 200 μL were mixed with the tested samples (0.1 mg/mL; 20 μL). Blank solutions were obtained by replacing the samples with the same volume of ethanol. Quercetin was employed as a positive control (0.4 mg/mL). The mixtures were incubated for 6 min, and the OD was measured at 734 nm. A calibration curve of Trolox (25 – 200 μM) was obtained. The results were elaborated by linear regression with the standard calibration curve ($R^2 = 0.9911$) and expressed as mg of TE per gram of PVS dry weight (mg TE/g DW).

2.6.4. α-Glucosidase inhibition

The α-glucosidase inhibition capacity of OPVS-E was evaluated *in vitro* using a 96-well microplate, following a previously described method (Cardullo, Floresta, Rescifina, Muccilli, & Tringali, 2021). OPVS-E was dissolved in methanol at 0.5 mg/mL. The amount of methanol used in the final experiment did not affect the glucosidase inhibitory activity. Different aliquots (2, 4, 6, 8, 10 μL) of OPVS-E were mixed with the α-glucosidase solution (100 μL of 0.25 U/mL in 50 mM phosphate buffer, pH 6.8). Afterwards, the substrate *p*-nitrophenyl-α-glucoside (78 μM; 100 μL) was pipetted into each well. The mixtures were kept under stirring at 37 °C for 30 min. The reaction was stopped by adding 1 M Na_2CO_3 solution (10 μL) and the optical density of *p*-nitrophenate released was measured at 405 nm using a Synergy H1 microplate reader. Acarbose and MeOH were used as positive control and blank, respectively. The % of inhibition was determined according to equation (4):

$$inhibition(\%) = \frac{(OD_{blank} - OD_{sample})}{OD_{blank}} \times 100 \quad (4)$$

The concentration required to inhibit 50 % of the enzyme activity (IC_{50}) was calculated by regression analysis using linear fitting, and it was expressed in μg/mL.

2.6.5. α-Amylase inhibition

The α-amylase inhibition assay followed a validated protocol (Cardullo, Floresta, et al., 2021), with slight modifications. Briefly, the enzyme solution (6 U/mL in 20 mM phosphate buffer; 50 μL) was mixed with different aliquots of the OPVS-E (2, 4, 6, 8 μL of a 0.2 mg/mL) and incubated at 37 °C for 10 min. Subsequently, a starch solution previously prepared by stirring at 90 °C for 20 min (0.5 % in water) was added. The mixtures were incubated at 37 °C for 15 min. Lastly, 96 mM 3,5-dinitrosalicylic acid solution (containing 30 % sodium potassium tartrate in 2 N NaOH) was added. All the reactants were heated at 80 °C for 10 min and diluted with MilliQ-water (300 μL). The mixtures were individually moved into a 96-well microplate, and the optical density was acquired at 540 nm. Acarbose was used as positive control, MeOH as blank. The results were obtained in quadruplicate. The percentage of inhibition was obtained according to equation (4) and regression analysis using linear fitting allowed to achieve the IC_{50} value (μg/mL).

2.7. Reactive oxygen species (ROS) scavenging assays

2.7.1. Superoxide radical anion ($O_2^{\bullet-}$) scavenging assay

The scavenging capacity of OPVS-E against the superoxide radical anion ($O_2^{\bullet-}$) was spectrophotometrically determined, following a

described method (Gomes et al., 2007). The sample was dissolved in phosphate buffer (19 mM; pH 7.4) and serial diluted from 500 to 15.62 μg/mL. Catechin, gallic acid, and Trolox were dissolved in the same phosphate buffer and used as positive control. The reactants were mixed into a 96-well microplate at the respective final concentrations as following: NADH (166 μM), NBT (43 μM), the tested sample/positive controls at different concentrations, and PMS (2.7 μM). The OD was measured at 560 nm for 2 min. Samples were assayed in triplicate and the results were expressed as concentration of sample needed to inhibit the $O_2^{\bullet-}$-induced NBT reduction in 50 % (IC_{50}, μg/mL).

2.7.2. Hypochlorous acid (HClO) scavenging assay

The ability of OPVS-E to inhibit the HClO-induced oxidation of DHR to rhodamine was investigated according to Pinto *et al.* (Pinto, Vieira, et al., 2021). Briefly, HClO was generated from a 1 % (*m/v*) NaOCl solution, by fixing the pH to 6.2, with dropwise addition of 10 % H_2SO_4. Subsequently, the HClO concentration was spectrophotometrically determined at 235 nm using the molar absorption coefficient of 100 M^{-1} cm^{-1} and the proper dilution was performed in phosphate buffer (100 mM; pH 7.4). The sample was previously dissolved in the same buffer and serial diluted from 7.81 to 0.97 μg/mL. Catechin, gallic acid and Trolox were employed as positive controls. Working solutions of 5 μM DHR in phosphate buffer were obtained from the stock solution immediately before the measurements and kept far from light. Each well of a 96-well microplate was filled with the following reagents: phosphate buffer solution (100 mM); tested sample and positive controls at different concentrations; DHR (5 μM) and HClO (5 μM). The OD was measured at the emission wavelength of 528 nm, with excitation at 485 nm. The results were obtained in triplicate and expressed as a percentage of inhibition, in IC_{50}, of HClO-induced oxidation of DHR.

2.7.3. Oxygen radical absorbance capacity (ORAC) assay

The antioxidant activity of OPVS-E towards the peroxyl ($ROO^{\bullet}$) radical was determined following the ORAC method described by Ou *et al.* (Ou, Hampsch-Woodill, & Prior, 2001), with slight modifications. Briefly, the sample was dissolved in phosphate buffer (75 mM; pH 7.5) and serial diluted from 15.62 to 0.48 μg/mL. 150 μL of a freshly prepared 61.2 nM fluorescein solution were added to each well of a 96-well microplate, followed by 25 μL of samples/positive controls (catechin and gallic acid) and 25 μL of AAPH solution 19.1 mM. Trolox was employed as standard (R^2 = 0.9863). Fluorescence was recorded at 37 °C every minute for 120 min (λ_{ex}: 485; λ_{em}: 528) and the decrease in fluorescence was monitored. A blank using phosphate buffer instead of sample was included in the assay. The ORAC values were calculated using the area under the fluorescence decay curves of extract/positive controls and expressed as μmol of TE per mg of PVS dry weight (μmol TE/mg DW).

2.8. HPLC/ESI-MS/MS analysis

The qualitative and quantitative determination of bioactive compounds in OPVS-E was carried out on an ion trap mass spectrometer equipped with an ESI ion source (LTQ, Thermo Fischer Scientific, San Jose, CA, USA) operating in negative mode. OPVS-E was previously dissolved in a mixture of MeOH/H_2O (50:50, *v/v*) at 20 mg/mL; 20 μL were loaded with the autosampler onto a Waters Symmetry RP-C18 column (150 mm × 1 mm i.d., 100 Å, 3.5 μm) heated at 25 °C. The mass spectrometer was coupled online with an LC pump (Dionex-Ultimate 3000, Thermo Fischer Scientific, San Jose, CA, USA). Elution was performed with the following gradient of H_2O + 1 % FA (solvent A) and ACN + 1 % FA (solvent B) at 50 μL/min: t_0 min B (5 %), t_{25} min B (15 %), t_{40} min B (25 %), t_{55} min B (55 %), t_{60} min B (95 %), t_{65} min B (100 %), t_{80} min B (5 %). Full scan mass spectra were acquired in negative ionization mode in the *m/z* range 150 – 2000. ESI ion source operated with 220 °C capillary temperature, 30 a.u., sheath gas, 4 kV source voltage and −18 V capillary voltage. Mass spectrometric analysis was performed by the data-dependent method with normalized collision energy of 29 a.u. and activation Q was set as 0.250. Mass calibration was achieved with a standard mixture of caffeine (Mr 194.1 Da), MRFA peptide (Mr 524.6 Da) and Ultramark (Mr 1621 Da). Data acquisition and analyses were performed with the Xcalibur v. 1.3 Software (Thermo Fischer Scientific, San Jose, CA, USA). Gallic acid derivatives and hydrolysable tannins were quantified using gallic acid as standard (0.1 – 6 × 10^{-4} mg/mL; $y = 1 \times 10^{-7}x + 96640$; $R^2 = 1$). Quercetin-3-*O*-glucoside was employed as standard to quantify flavonoids (0.1 – 4.2 × 10^{-3} mg/mL; $y = 2 \times 10^{8}x + 1 \times 10^{7}$; $R^2 = 0.9969$), whereas fatty acids and anacardic acids were quantified as (17:1)-anacardic acid (0.12 – 6.3 × 10^{-4} mg/mL; $y = 1 \times 10^{8}x + 2 \times 10^{6}$; $R^2 = 0.998$). The results obtained were expressed as mg of organic compound per gram of PVS dry weight (mg/g DW).

2.9. In vitro cell assays

2.9.1. Cell lines and culture conditions

Two different types of human colon epithelial cells, namely HT29-MTX and Caco-2, were cultured in DMEM supplemented with 0.25 μg/mL amphotericin B, 1 % (*v/v*) of antibiotic–antimitotic mixture (final concentration of 100 U/mL penicillin and 100 μg/mL streptomycin), 1 % (*v/v*) L-glutamine, 10 % (*v/v*) inactivated FBS and 1 % (*v/v*) of non-essential amino acids. Cells were incubated at 37 °C in a cell culture incubator (CellCulture® CO_2 Incubator, ESCO GB Ltd, UK) in a 5 % CO_2 environment and under a water saturated atmosphere until confluence. Caco-2 clone type C2BBe1 were obtained by American Type Culture Collection (ATCC Number: HTB-37, Manassas, VA, USA; Caucasian ethnicity; 72 years old; male gender; colon tissue). HT29-MTX were supplied by ATCC (ATCC Number: HTB-38; ATCC, Manassas, VA, USA; Caucasian ethnicity; 44 years old; female gender; colon tissue).

2.9.2. Cell viability assay

An MTT (3-(4,5-dimethylthiazol-2-yl)-2,5-diphenyltetrazolium bromide) colorimetric assay was carried out to assess the effects of OPVS-E towards the two human intestinal cell lines (Caco-2 and HT29-MTX), according to Silva *et al.* (Silva et al., 2022). Two freshly prepared solutions containing Caco-2 cells (passage 12 – 13) and HT29-MTX cells (passage 46 – 47) were prepared in DMEM at 1 × 10^5 cells/mL and incubated into a 96-well microplate for 48 h. OPVS-E was dissolved in the same DMEM medium, diluted in concentrations ranging from 62.5 to 1000 μg/mL, and put in contact with cells for 24 h. DMEM and 1 % (*w/v*) Triton X-100 were treated as samples and used as positive and negative control, respectively. After 24 h of incubation, OPVS-E was removed, and the cells were washed with HBSS. MTT reagent (0.5 %, *w/v*) was added, and the plate was incubated for 3 h at 37 °C, protected from light. DMSO was used to dissolve the insoluble purple formazan product. Afterwards, the cell viability was quantitatively determined reading the OD at 570 nm, with a background subtraction at 690 nm. Results were expressed as percentages of cell viability.

2.10. Statistical analysis

All experiments were performed at least in triplicate, and the results were expressed as mean ± standard deviation. The statistical analyses were performed using the OriginPro 2023 software (Northampton, Massachusetts, USA) and One-way ANOVA. Differences between samples were denoted as statistically significant when *p*-values were lower than 0.05 ($p < 0.05$), according to Tukey's test.

3. Results and discussion

3.1. Single-factor experiments

In single-factor experiments, four critical factors were identified as significant contributors to the MAE from PVS, namely ethanol in water

Table 1
Results of the single-factor experiments for PVS.

EtOH conc. (X_1) (% v/v)	TPC yield	Extraction time (X_2) (s)	TPC yield	MW power (X_3) (W)	TPC yield	Solvent-to-solid ratio (X_4) (mL/g)	TPC yield
20	11.21 ± 0.89^{b}	50	10.56 ± 0.45^{c}	150	11.52 ± 0.88^{c}	20	11.59 ± 0.16^{b}
50	13.50 ± 0.87^{a}	90	10.78 ± 0.66^{b}	430	15.52 ± 0.37^{b}	25	12.74 ± 0.22^{a}
80	13.82 ± 1.09^{a}	120	13.68 ± 0.23^{b}	670	16.66 ± 0.62^{ab}	30	10.92 ± 0.49^{b}
90	10.21 ± 0.69^{b}	210	14.77 ± 0.98^{ab}	850	18.26 ± 0.49^{a}	35	10.86 ± 0.35^{b}
		270	15.79 ± 0.41^{a}	1000	16.54 ± 0.86^{b}		

Data are expressed as mg of gallic acid equivalents per g of PVS dry weight (mg GAE/g DW) and reported as means ± standard deviation ($n = 4$). Different letters in the same column indicate significant differences (Tukey's test, $p < 0.05$).

concentration (X_1), irradiation time (X_2), MW power (X_3), and solvent-to-solid ratio (X_4). Firstly, the extractions were conducted by varying one parameter at a time, while maintaining the others at fixed central values (50 % EtOH, 430 W, 120 s, and 25 mL/g). An overview of all factor levels investigated in this study can be found in **Table S1**. Subsequently, an assessment of the total phenolic content (TPC) in the extracts was performed to establish preliminary parameter ranges for optimization in the experimental design phase.

As indicated in Table 1, the initial factor ranges chosen for the development of the optimization model were as follows: 20 %, 50 %, and 80 % (*v/v*) for ethanol concentration; 120 s, 210 s, and 270 s for extraction time; 670, 850, and 1000 for MW power; and 20 mL/g, 25 mL/g, and 30 mL/g for the solvent-to-solid ratio.

As can be observed in Table 1, the TPC yield increased from 11.21 mg GAE/g DW to 13.82 mg GAE/g DW by raising the ethanol concentration up to 80 % and then, substantially decreased to a higher concentration (90 %). A similar trend was observed by Dahmoune *et al.* for the MAE of polyphenols from *Myrtus communis* L. leaves (Dahmoune, Nayak, Moussi, Remini, & Madani, 2015). Consequently, the optimization design explored the ethanol concentration between 20 and 80 %. A solvent mixture with 50 % of ethanol in water was used to determine the preliminary range of the other extraction variables investigated in this study.

Irradiation time is another factor that undoubtedly influences the MAE process. This latter was initially modified from 50 to 270 s. A significant increase in the recovery of polyphenols (from 10.56 to 15.79 mg GAE/g DW) was observed by increasing the irradiation time. Although a shorter time is desirable to reduce the energy costs and prevent thermolabile compounds from degradation, 50 and 90 s were insufficient to provide a good sample heating (Lopez-Salazar, Camacho-Diaz, Ocampo, & Jimenez-Aparicio, 2023). Therefore, 120 – 270 s was the selected preliminary range for the irradiation time.

Another set of extractions was carried out by changing the MW power from 150 to 1000 W, keeping the ethanol concentration constant at 50 % for 120 s, with a solvent-to-solid ratio of 25 mL/g. It was observed that the TPC yield increased at higher MW powers. A similar behaviour was reported by Sanchez-Reinoso *et al.* for MAE of *Sacha inchi* shells (Sanchez-Reinoso, Mora-Adames, Fuenmayor, Darghan-Contreras, Gardana, & Gutierrez, 2020). Hence, 670, 850, and 1000 W were the MW powers selected for the experimental design.

Lastly, considering a potential industrial scale-up of this process, it is fundamental to establish the solvent-to-solid ratio to recover the maximum of bioactive compounds. In this single-factor trial, it was observed that the TPC decreased (from 12.74 to 10.86 mg GAE/g_{dw}) as the solvent–to-solid ratio increased from 25 to 35 mL/g, due to a reduced stirring of the sample at higher ratios. According to these findings, the range 20 – 30 mL/g was selected for the optimization. **Table S2** summarizes all the preliminary ranges selected in this study to design the following MAE experiments.

3.2. Model fitting and experimental design

BBD was employed to evaluate the influence of the four independent variables (X_1 – X_4) on the dependent responses (Y_1 = TPC; Y_2 - Y_4 = antioxidant/antiradical activities), optimizing the MAE conditions for the maximum recovery of bioactive compounds from PVS. Table 2 summarizes the MAE experiments conducted with the different factor combinations and the corresponding results in terms of TPC and antioxidant/antiradical capacities evaluated by FRAP, DPPH, and ABTS assays. As can be observed in Table 2, the TPC ranged from 9.60 (run 17) to 20.57 mg GAE/g DW (run 20); the FRAP values varied from 2.91 (run 26) to 5.80 mg TE/g DW (run 15); the DPPH results ranged between 76.15 (run 2) and 107.16 μg TE/g DW (run 20); and the ABTS values varied from 9.81 (run 2) to 17.50 mg TE/g DW (run 20).

Once performed the experimental design, the regression analysis was provided by the model using the least square technique (Weremfo et al., 2023), as detailed in Table 3.

According to Table 3, all the linear coefficients were highly significant at the level of $p < 0.05$. Moreover, the ethanol concentration (X_1) presenting *F*-values of 57.32 for TPC, 95.30 for FRAP, 54.01 for DPPH, and 106.11 for ABTS, constituted the factor that affected the TPC and antioxidant/antiradical activities of PVS. The model was highly significant ($p < 0.0001$) for all responses (TPC, FRAP, DPPH, and ABTS), with *F*-values of 10.41, 13.30, 7.80, and 22.85, respectively. R^2 values close to 1 highlight a high correlation between the measured and the predicted values. Additionally, the lack of fit was not significant, indicating the model suitability in determining the optimal parameters. The model adequacy was further confirmed by the coefficient of variation (CV). Usually, CV < 10 is desirable to ensure the reliability and not significant variability of the collected experimental data (Bezerra, Santelli, Oliveira, Villar, & Escaleira, 2008) (Dahmoune et al., 2015). The CV value of our model was 2.62 %, meaning that all the measurements carried out to develop the experimental design were consistent. The final predictive polynomial equations, representing the empirical relationship between each response and all the factors investigated, are summarized in Eq. (5) – (8):

$$Y_1(TPC) = 107.0920 + 0.1059x_1 + 0.3841x_2 + 0.0498x_3 + 4.6564x_4 - 0.0002x_2^2 \quad (5)$$

$$Y_2(FRAP) = 4.9354 + 0.0703x_1 + 0.0683x_2 - 0.0108x_3 + 0.3982x_4 + 8.86 \times 10^{-6}x_3^2 + 0.0033x_4^2 - 4.75 \times 10^{-5}x_1x_3 - 0.0022x_1x_4 - 4.09 \times 10^{-5}x_2x_3 - 0.0014x_2x_4 + 0.0003x_3x_4 \quad (6)$$

$$Y_3(DPPH) = -247.1938 + 0.1325x_1 + 0.2791x_2 + 0.2535x_3 + 14.9858x_4 - 0.1596x_4^2 - + 9.62 \times 10^{-5}x_1x_3 - 0.0207x_1x_4 - 0.0003x_2x_3 - 0.0062x_3x_4 \quad (7)$$

Table 2
Experimental design and results of the TPC and antioxidant/antiradical activities of PVS extracts evaluated by FRAP, DPPH, and ABTS.

Run	Independent variables				Dependent variables			
	MAE conditions				Experimental values			
	X_1 (EtOH, % v/v)	X_2 (Time, s)	X_3 (MW, W)	X_4 (Ratio, mL/g)	Y_1, TPC (mg GAE/g DW)	Y_2, FRAP (mg TE/g DW)	Y_3, DPPH (μg TE/g DW)	Y_4, ABTS (mg TE/g DW)
1	50	210	850	25	15.18 ± 1.14	3.96 ± 0.66	94.92 ± 1.86	12.25 ± 0.34
2	50	210	670	20	11.61 ± 0.18	4.33 ± 1.20	76.15 ± 1.97	9.81 ± 0.10
3	20	270	850	25	17.46 ± 0.47	4.71 ± 0.45	100.42 ± 1.15	16.54 ± 0.41
4	80	120	850	25	13.82 ± 1.23	3.90 ± 0.64	85.99 ± 2.51	12.73 ± 0.71
5	50	270	850	30	10.81 ± 0.46	4.20 ± 0.56	93.46 ± 1.24	14.49 ± 1.15
6	50	210	670	30	16.27 ± 0.43	4.34 ± 0.64	95.78 ± 1.39	14.69 ± 0.55
7	50	270	670	25	15.66 ± 0.06	4.14 ± 0.49	92.63 ± 1.64	13.79 ± 0.49
8	20	210	850	20	14.98 ± 0.18	4.55 ± 0.24	89.68 ± 1.45	13.08 ± 0.32
9	50	210	850	25	15.17 ± 0.74	3.98 ± 0.43	93.01 ± 1.83	12.75 ± 0.66
10	80	210	1000	25	14.39 ± 0.71	3.28 ± 0.19	90.15 ± 1.16	13.10 ± 0.82
11	80	210	850	20	12.20 ± 0.70	3.01 ± 0.28	79.58 ± 1.68	13.20 ± 0.32
12	50	270	850	20	13.63 ± 0.21	4.40 ± 0.60	80.71 ± 0.89	12.80 ± 0.78
13	80	210	670	25	12.23 ± 0.54	4.02 ± 0.62	81.72 ± 1.27	12.55 ± 0.64
14	50	270	1000	25	13.13 ± 0.07	4.32 ± 0.23	98.94 ± 1.48	14.61 ± 0.71
15	20	210	850	30	17.21 ± 1.39	5.80 ± 0.51	99.67 ± 1.71	17.36 ± 0.55
16	50	120	850	30	16.60 ± 1.19	5.23 ± 0.42	96.41 ± 1.78	15.05 ± 0.14
17	50	120	670	25	9.60 ± 0.36	4.03 ± 0.57	78.20 ± 1.60	12.33 ± 0.47
18	50	120	1000	25	16.40 ± 0.55	5.17 ± 0.46	99.31 ± 1.24	14.42 ± 0.36
19	50	210	1000	30	14.53 ± 0.70	4.59 ± 0.39	98.03 ± 1.93	14.66 ± 0.56
20	20	210	1000	25	20.57 ± 0.92	5.14 ± 0.62	107.16 ± 1.72	17.50 ± 0.41
21	20	120	850	25	18.57 ± 0.55	4.90 ± 0.52	106.03 ± 1.81	15.78 ± 0.46
22	20	210	670	25	16.57 ± 0.02	4.96 ± 0.45	100.69 ± 1.45	14.42 ± 0.70
23	50	210	850	25	15.43 ± 0.59	3.95 ± 0.66	95.64 ± 2.27	12.21 ± 0.49
24	80	270	850	25	11.75 ± 0.47	3.59 ± 0.23	79.33 ± 1.40	12.94 ± 0.91
25	50	210	1000	20	14.52 ± 0.22	3.73 ± 0.15	98.54 ± 0.52	14.14 ± 0.58
26	80	210	850	30	11.74 ± 0.88	2.91 ± 0.18	77.11 ± 1.69	10.22 ± 0.22
27	50	120	850	20	10.85 ± 0.62	3.39 ± 0.12	91.21 ± 0.81	11.50 ± 0.29

Table 3
Results of ANOVA from the BBD model for TPC (Y_1) and antioxidant/antiradical activities evaluated by FRAP (Y_2), DPPH (Y_3), and ABTS (Y_4) assays for PVS.

Variable	Sum of squares				*F*-value				*p*-value			
	Y_1	Y_2	Y_3	Y_4	Y_1	Y_2	Y_3	Y_4	Y_1	Y_2	Y_3	Y_4
Model	163.06	12.53	136.20	87.60	10.41	13.30	7.80	22.85	< 0.0001*	< 0.0001*	< 0.0001*	< 0.0001*
X_1	64.12	6.41	949.35	29.06	57.32	95.30	54.01	106.11	0.0102*	< 0.0001*	< 0.0001*	< 0.0001*
X_2	5.77	0.59	106.05	1.75	32.00	8.01	6.34	5.83	< 0.0001*	0.0109*	0.0460*	0.0397*
X_3	18.80	0.48	431.28	10.83	16.80	7.06	24.54	39.55	0.0003*	0.0268*	0.0003*	< 0.0001*
X_4	14.48	1.45	163.19	13.76	12.94	21.59	9.28	50.26	0.0037*	0.0005*	0.0101*	< 0.0001*
X_1*X_2	0.16	0.03	0.004	0.07	0.15	0.41	0.02	0.28	0.7091	0.5326	0.9878	0.6066
X_1*X_3	6.78	1.82	8.13	1.63	5.70	3.32	0.52	4.78	0.0186*	0.0433*	0.0007*	0.0097*
X_2*X_3	23.30	1.06	75.03	0.32	20.83	15.75	5.27	5.96	0.0007*	0.0018*	0.0411*	0.0310*
X_1*X_4	5.82	0.53	104.30	5.93	5.20	7.94	5.93	21.64	0.0416*	0.0154*	0.0313*	0.0005*
X_2*X_4	17.89	1.09	11.28	1.14	16.00	16.31	0.64	4.17	0.0018*	0.0016*	0.4386	0.0637
X_3*X_4	1.80	0.45	38.73	13.15	1.61	6.72	2.20	48.01	0.2281	0.0234*	0.1634	< 0.0001*
X_1*X_1	2.41	0.01	13.98	6.87	2.15	0.17	0.79	25.10	0.1682	0.6852	0.3899	0.0003*
X_2*X_2	5.57	0.18	7.05	4.12	4.98	2.77	0.40	15.04	0.0455*	0.1216	0.5384	0.0022*
X_3*X_3	0.01	0.58	10.01	3.82	0.12	8.56	0.57	13.96	0.9734	0.0127*	0.4651	0.0028*
X_4*X_4	10.42	1E-03	97.16	0.09	9.31	0.01	5.53	0.35	0.0101*	0.9424	0.0366*	0.5643
Lack of fit	0.73	0.06	0.05	0.18	4.39	0.84	0.74	0.75	0.9050	0.0742	0.0848	0.7722
R^2	0.92	0.94	0.90	0.96								
R^2 (Adj.)	0.83	0.87	0.78	0.92								

X_1: solvent concentration (%, *v/v*); X_2: irradiation time (*s*); X_3: MW power (W); X_4: solvent-to-solid ratio (mL/g).
* Values statistically significant at $p < 0.05$.

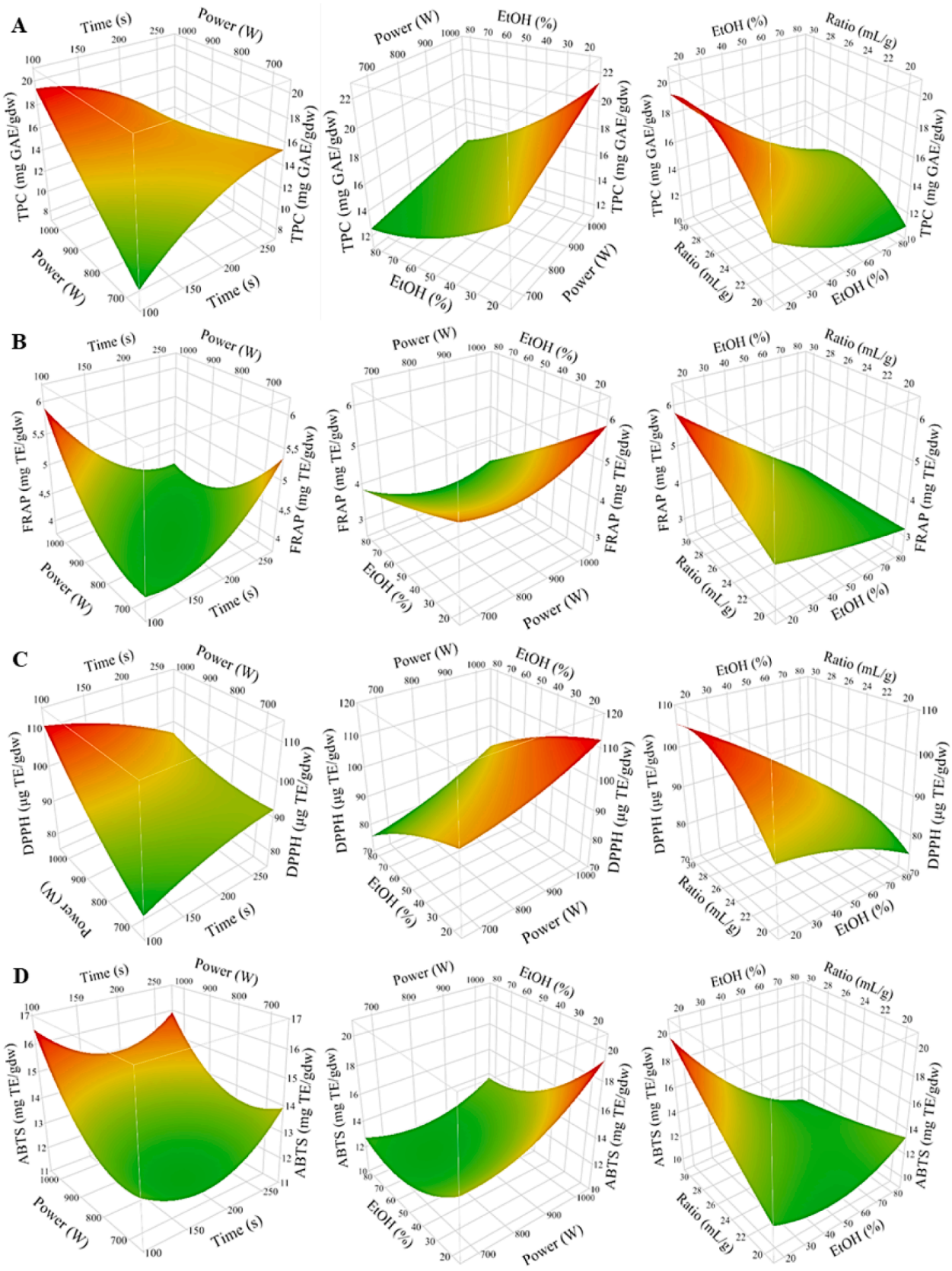

Fig. 1. 3-D response surfaces plots for TPC (A), FRAP (B), DPPH (C), and ABTS (D) as a function of the significant interaction terms (irradiation time/MW power; MW power/ethanol concentration; ethanol concentration/solvent-to-solid ratio).

$$Y_4(ABTS) = -16.0788 + 0.2293x_1 - 0.0412x_2 + 0.0009x_3 + 1.7680x_4 + 0.0013x_1^2 + 1.64 \times 10^{-4}x_2^2 + 3.14 \times 10^{-5}x_3^2 + 0.0054x_4^2 - 1.28 \times 10^{-4}x_1x_3 - 0.0121x_1x_4 - 2.25 \times 10^{-5}x_2x_3 - 0.0015x_3x_4 \quad (8)$$

3.3. Analysis of the response surfaces (RSM)

The RSM represents a powerful statistical tool to account for the mutual interactions among all variables included in the optimization design (Bonaccorso et al., 2021). Precisely, the effects of two paired factors on the responses investigated can be easily visualized by 3D-response surface plots, resulting from the model equations mentioned above.

Fig. 1 **A - D** illustrates the effects of the significant interaction terms on TPC (Fig. 1A), FRAP (Fig. 1B), DPPH (Fig. 1C), and ABTS (Fig. 1D) assays. The 3-D response surface plots observed for the not significant interaction terms (X_1X_2, X_3X_4, and X_2X_4) are reported in **Figure S1**.

Overall, all four response variables presented a similar trend in the response surfaces.

Concerning the mutual effect between the MW power and the irradiation time (X_2X_3 interaction term) on the response variables, it can be observed that both TPC and antioxidant/antiradical activities increased employing a short irradiation time (around 100 s) at a high MW power (1000 W). This pattern might be linked to the increased solubility of compounds at elevated temperatures. Typically, high microwave (MW) power levels lead to increased temperatures, causing a higher migration of compounds from the shell matrix to the solvent (Dahmoune et al., 2015). At the same time, shorter exposure times could shield specific compounds from thermal breakdown, which could clarify the h high responses observed with this combination of factors. Other studies also reported that the MAE of phenolic compounds was effective with low irradiation times and high MW powers, suggesting a common trend with the present study (Dahmoune, Boulekbache, Moussi, Aoun, Spigno, & Madani, 2013; Hiew, Lee, Junus, Tan, Chai, & Ee, 2022).

According to Table 3, the mutual interaction between the MW power and the ethanol concentration (X_1X_3 interaction term) was significant for all the response variables. Specifically, the shape of the response surfaces indicates that both TPC and antioxidant/antiradical activity increased as the MW power increased, with an ethanol concentration between 20 and 30 %. This combination of factors leads to enhanced extraction efficiency, likely because of increased sample swelling induced by water, consequently facilitating greater migration of compounds from the sample matrix into the solvent. (Dahmoune et al., 2015). Fig. 1 **A - D** shows that when the solvent-to-solid ratio increased from 26 to 30 mL/g, always within 20 – 30 % of ethanol, the ethanol, the TPC and the antioxidant/antiradical activity increased as well. This trend could be attributed to a higher concentration gradient in presence of higher amount of solvent, which leads to a higher compound diffusion rate (Hiew et al., 2022).

3.4. Selection of the optimal MAE conditions and model validation

According to the final predictive equations and the regression analysis reported above, the optimal calculated MAE conditions for the highest TPC were 20 % EtOH, 120 s, 1000 W, and 30 mL/g. The predicted optimal conditions for FRAP were 20 % EtOH, 135 s, 1000 W, and 27.9 mL/g; for DPPH were 20 % EtOH, 135 s, 1000 W, and 25.09 mL/g; and for ABTS were 20 % EtOH, 135 s, 1000 W, and 27.7 mL/g. Consequently, 20 % EtOH, 135 s, 1000 W, and 27.7 mL/g were the optimal MAE conditions selected for this study. Under this factor combination, the expected value for the TPC was 23.15 mg GAE/g DW, with FRAP value of 7.35 mg TE/g DW, DPPH 113.29 μg TE/g DW and ABTS 20.12 mg TE/g DW. The optimal predicted factor combination was experimentally validated by performing a MAE extraction in triplicate (OPVS-E) to verify the model's predictions. **Table S3** compares the predicted and the obtained values of TPC and *in vitro* antioxidant/antiradical activities of OPVS-E. The experimental and the predicted results agreed each other, and no significant variance ($p < 0.05$) was observed between the values (**Table S3**).

The OPVS-E showed a TPC value of 23.83 mg GAE/g DW, which resulted higher than the corresponding TPC values of 11.23 mg GAE/g DW obtained from the ultrasound-assisted extraction of phenolics from hazelnut shells (Yuanu, Lu, Eskridge, & Hanna, 2018) and 8.49 mg GAE/g DW from a walnut shell extract obtained by MAE (Muccilli et al., 2023).

Concerning the antioxidant activity, the OPVS-E exhibited an ABTS value of 20.55 mg TE/g DW), which was higher than the one reported for an hydroalcoholic extract from *Juglans regia* L. shells (2.88 mg TE/g DW) obtained by MAE (Muccilli et al., 2023).

Furthermore, an extraction yield of 13.6 % (*w/w*; g of dry extract over 100 g of PVS) was achieved under the optimal conditions. This extraction yield was comparable to the one reported for the alcoholic extract from *Castanea sativa* shells (13.02 %) obtained by MAE (Pinto, Silva, Freitas, Vallverdú-Queralt, Delerue-Matos, & Rodrigues, 2021). A lower extraction yield (3 % *w/w*) was reported by Cardullo *et al.* for a pistachio shell extract obtained using ethanol and a MW power of 1000 W for 270 s (Cardullo, Leanza, et al., 2021), highlighting the importance of RSM to achieve the optimal extraction parameters to recover bioactive compounds from agro-industrial by-products.

3.5. Phytochemical composition of OPVS-E

HPLC/ESI-MS/MS analysis allowed to obtain information about the complex phytochemical composition of the OPVS-E. Fig. 2 shows the total ion current (TIC) chromatogram obtained in negative ionization mode. The main constituents of the extract were tentatively identified by comparing the mass spectrometric data with the literature. The tentatively identified compounds were progressively numbered according to their HPLC/ESI-MS retention times and listed in Table 4. For each compound, $[M - H]^-$ *m/z* values, the main MS/MS fragments and the relative abundances are reported as well.

52 compounds were tentatively identified in OPVS-E. Their chemical structures are shown in **Figure S2**. Specifically, four classes of compounds were distinguished, namely gallic acid derivatives, including hydrolysable tannins (**3** – **5**, **7**, **8**, **10**, **15**, **20**, **22**, **24**, **25**), flavonoids (**6**, **9**, **11** – **14**, **16** – **19**, **21**, **26**, **27**, **31**), fatty acids (**23**, **28** – **30**, **32** – **40**, **44**, **45**) and anacardic acids (**41** – **43**, **46** – **52**). The constituents of the OPVS-E eluted as not overlapping peaks were quantified by HPLC-MS employing as reference standards gallic acid for compounds **10**, and **22**; quercetin-3-*O*-glucoside for **6**, **14**, and **31**; and (17:1)-anacardic acid for **23**, **28**, **30**, **32**, **33**, **37**, **42**, **47**, **48.** Coeluting compounds (**18** + **19**, **26** + **27**, **44** + **45**, **49** + **50**) were quantified together. The detailed MS/MS data interpretation are reported in **Supplementary Material**.

Gallic acid derivatives, hydrolysable tannins and flavonoids eluted at the beginning of the TIC chromatogram (t_r = 10.90 – 27.70 min) with compounds **8**, **10**, **14**, **19** constitute the most abundant phenolic components of the extract (Table 4). Several saturated and unsaturated fatty acids appeared in intense peaks between t_r = 38.45 – 65.80 min (Fig. 2) except for compound **23** tentatively identified as the glycoside of **39** and eluting at 23.8 min. Their tentative identifications were achieved by comparing their MS/MS data with the information retrieved from LIPID

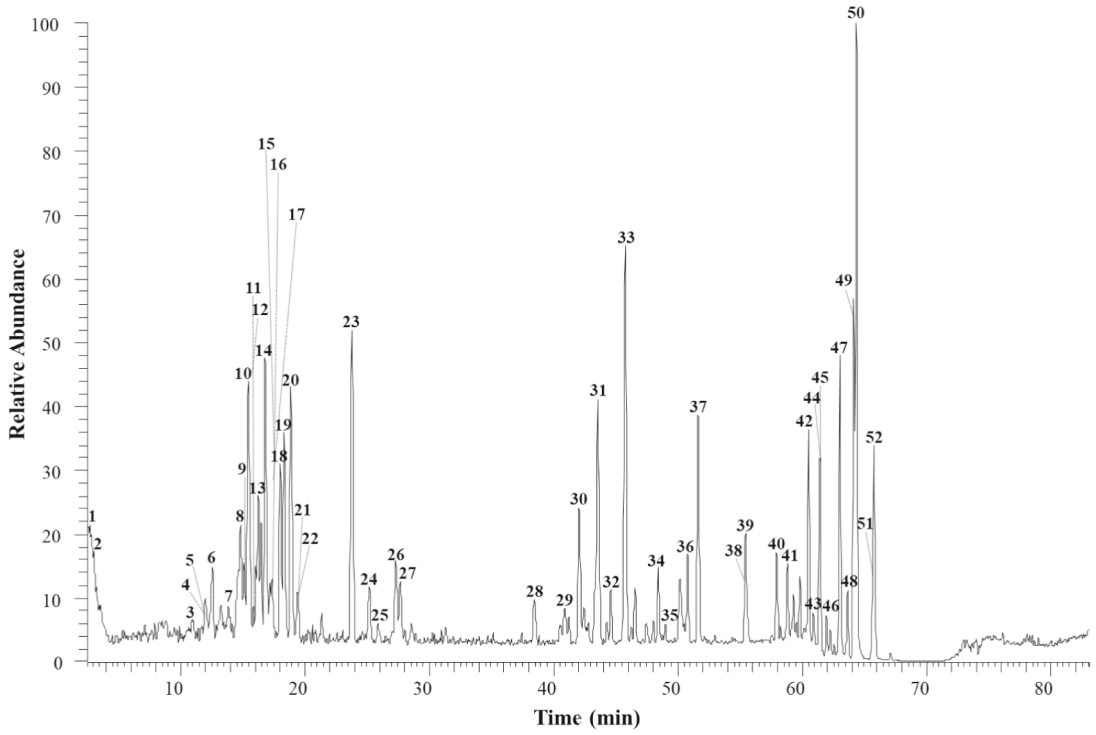

Fig. 2. HPLC/ESI-MS/MS profile (negative mode) of OPVS-E. Peaks' identifications are shown in Table 4.

MAPS® Structure Database (LMSD) (Sud et al., 2007).

Anacardic acids (**49**, **50** and **52**) were identified among the most abundant constituents of the extract. The presence of this group of natural products has been previously documented in cashew nut shells (Jerz, Murillo-Velasquez, Skrjabin, Gök, & Winterhalter, 2011), as well as in red and green pistachio hulls (Erşan, Üstündağ, Carle, & Schweiggert, 2016). However, to the best of our knowledge, this is the first study that reports the occurrence of anacardic acids in pistachio shells. Anacardic acids have been studied for their potential health benefits, including antioxidant, anti-inflammatory and anti-bacterial properties (Morais et al., 2017). Moreover, Toyomizu *et al.* reported a strong inhibitory activity of anacardic acids towards α-glucosidase and aldose reductase, key hydrolytic enzymes involved in carbohydrate absorption (Toyomizu, Sugiyama, Jin, & Nakatsu, 1993).

3.6. Hypoglycaemic activity of OPVS-E

The OPVS-E potential inhibitory effect towards both α–glucosidase (from *Saccharomyces cerevisiae*) and porcine pancreatic α–amylase was evaluated for the first time in this study. Table 6 reports the extract concentration (μg/mL) required to inhibit in 50 % the enzymatic activity (IC_{50}) when compared to the anti-diabetic drug acarbose. The OPVS-E showed a notable α-glucosidase inhibitory activity (IC_{50} = 41.07 μg/mL), which was much higher than the one observed for acarbose (IC_{50} = 98.34 μg/mL). Similarly, the extract achieved an IC_{50} of 2.05 μg/mL, resulting in a stronger α –amylase inhibitor than acarbose (IC_{50} = 8.93 μg/mL).

It is worth noting that a commercial tannin extract derived from *Schinopsis lorentzii* wood displayed weaker inhibitory effect when compared to OPVS-E (α-glucosidase: IC_{50} = 48.9 μg/mL;α-amylase:IC_{50} = 129.3 μg/mL (Cardullo, Muccilli, Cunsolo, & Tringali, 2020). Whereas, similarly to this study, chestnut (*Castanea mollissima* Blume) exocarps by-product, extracted by subcritical water extraction (SWE), exhibited promising α-glucosidase (IC_{50} = 12 μg/mL) and α-amylase (IC_{50} = 17 μg/mL) inhibitory activities, higher than those observed for acarbose (Liu et al., 2020). This emphasizes the remarkable achievements in utilizing agricultural by-products, like pistachio shells, as a potential source of hypoglycaemic agents.

The promising hypoglycaemic activity observed for the OPVS-E may be related with the main constituents, namely flavonoids, hydrolysable tannins, and anacardic acids. Different authors have reported the α-glucosidase and α-amylase inhibitory activities of flavonoids and hydrolysable tannins (Cardullo, Muccilli, Pulvirenti, et al., 2020; Lim, Ferruzzi, & Hamaker, 2022).

Despite limited knowledge surrounding anacardic acids, Toyomizu et al. characterized these compounds as potent inhibitors of α-glucosidase. (Toyomizu et al., 1993).

3.7. ROS scavenging capacity of OPVS-E

Previous studies have shown that chronic hyperglycemia induces excessive ROS production and an oxidative stress condition (Fiorentino et al., 2013). It is also well established that oxidative stress leads to cellular and tissue damage, favouring the deterioration of diabetes toward the appearance of complications such as diabetic vasculopathy (Ullah et al., 2016). Antioxidant-enriched extracts could be used to counteract the ROS overproduction that occurs during diabetes, interrupting the disease progression. Therefore, OPVS-E scavenging capacity against superoxide radical ($O_2^{\bullet -}$), hypochlorous acid (HClO), and peroxyl radical ($ROO^{\bullet}$) was screened (Table 6**)**. The OPVS-E showed its highest antiradical power against HClO, with an IC_{50} value of 4.70 μg/mL, which was not significantly ($p > 0.05$) different from gallic acid (IC_{50} = 5.51 μg/mL), used as positive control. This result was higher than the one reported by Pinto *et al.* for the ethanolic extract obtained from *Castanea sativa* Mill. shells by MAE (IC_{50} = 23.08 μg/mL) (Pinto, Silva, et al., 2021).

In what concerns to $O_2^{\bullet -}$, an IC_{50} of 54.92 μg/mL was obtained for the OPVS-E. This result was lower than the ones achieved for the controls used, respectively catechin (IC_{50} = 26.24 μg/mL) and gallic acid (IC_{50} = 10.39 μg/mL). Nevertheless, the OPVS-E showed a higher $O_2^{\bullet -}$ quenching capacity than the one reported by Ferreira *et al.* for the extract from *C. sativa* Mill. shells prepared by SWE at 180 °C (IC_{50} = 73.18 μg/mL)

Table 4
Tentative identification and quantification by HPL/ESI-MS/MS of the main organic constituents of OPVS-E.

Peak	t_r	$[M-H]^-$	Fragments, m/z (Relative intensity)	Proposed identification	mg/g DW of extract
1	2.50	133	115(100); 87(5)	Malic acid	
2	3.70	191	111(100); 173(40); 147(5)	Quinic acid	
3	10.9	183	168(100); 124(40)	Methyl gallate	
4	12.0	321	169 (100); 125(10)	Digallic acid	
5	12.0	481	463(100); 437(40) 301(40) 169(2)	HHDP-hexose isomer	
6	12.6	451	433(100); 292(20); 173(10); 337(5)	3-Hydroxyphloretin-O-glucoside (Aspalathin)	0.251 ± 0.009[b]
7	14.0	373	169(100); 313(80); 151(25)	Acetyl-O-galloyl hexose	
8	14.9	635	423(100); 465(80); 483(70); 313(20)	Tri-O-galloyl-glucose isomer	2.176 ± 0.023[a]
9	15.0	631	479(100); 317(15); 299(5); 271(5)	Myricetin galloyl hexoside	
10	15.5	197	169(100); 125(5)	Ethyl gallate	2.328 ± 0.023[a]
11	16.1	479	317(100); 359(5); 461(5); 271 (5); 179(5)	Myricetin hexoside	
12	16.1	625	316(100); 317(90); 607(20); 271(15); 463(10); 287(10)	Myricetin rhamno-hexoside	
13	16.3	493	317(100); 331(5); 211(5)	Myricetin hexuronide	
14	16.8	615	463(100); 301(80); 313(20); 453(5)	Quercetin galloyl hexoside isomer	1.009 ± 0.037[b]
15	17.4	787	617(100); 635(85); 465(10)	Tetragalloyl glucose isomer	
16	17.4	303	285(100); 125(10)	Taxifolin	
17	17.8	609	301(100); 300(50); 271(10); 463(5); 255(5); 179(5);	Quercetin-O-hexosedeoxyhexoside	
18	18.0	463	301(100); 179(5); 271(5); 255(5);	Quercetin hexoside	1.267 ± 0.033[b*]
19	18.4	477	301(100); 179(5); 151(5)	Quercetin monoglucuronide	1.267 ± 0.033[b,*]
20	18.9	319	239 (100); 139(5), 275(5)	Luteic acid	
21	19.4	433	301(100); 179(5); 343(10); 272(5)	Quercetin pentoside	
22	19.4	939	769(100); 787(15); 617(15); 635(5); 465(5)	Pentagalloyl glucose isomer	0.578 ± 0.021[a]
23	23.8	427	265(100); 247(5); 221(5)	Fatty acyl glycoside	2.724 ± 0.002[c]
24	25.2	347	267(100); 169(10)	Gallic acid derivative	0.673 ± 0.007[a]
25	25.2	483	321(100); 277(30); 271(10); 465(5); 331(5); 313(5); 169(5)	Digalloyl hexose	0.176 ± 0.013[a]
26	27.3	301	179(100); 151(90); 257(50); 273(30); 229(20); 283(20)	Quercetin	0.661 ± 0.035[b,ç]
27	27.7	285	241(100); 199(40); 151(25); 175(20)	Kaempferol	0.661 ± 0.035[b,ç]
28	38.5	327	229(100); 291(50); 211(50), 171(40), 227(20), 165(10)	(18:2) Trihydroxy-octadecadienoic acid isomer	0.359 ± 0.014[c]
29	41.0	331	313(100); 311(20); 295(20); 231(5)	(18:0) Trihydroxy-octadecanoic acid isomer	
30	42.1	329	229(100); 311(30) 171(10); 125(5)	(18:1) Trihydroxy-octadecenoic acid isomer	1.143 ± 0.027[c]
31	43.6	287	269(100); 155(10); 251(10)	Dihydrokaempferol	1.203 ± 0.016[b]
32	44.7	475	395(100); 431(20)	(32:2) Octadecanoid acid isomer	0.351 ± 0.008[c]
33	45.8	279	235(100); 217(60); 261(5); 252(5)	(18:2) Linoleic acid	3.192 ± 0.024[c]
34	48.5	393	313(100); 349(20); 375(10); 329(5)	(26:1) Hexacosenoic acid	
35	49.0	293	249(100); 193(90); 181(5)	(19:2) Octadecadienoic acid isomer	
36	50.8	395	351(100); 349(40); 315(60); 377(10); 283(10); 219(10)	(26:0) Hexacosanoic acid isomer	
37	51.6	307	263(100); 245(60); 246(10); 289(5)	(20:2) Eicosadienoic acid isomer	1.626 ± 0.030[c]
38	55.3	297	183(100); 197(40); 171(5); 253(5)	(18:1; O) Epoxyoctadecanoic acid isomer	
39	55.5	265	97(100); 238(40); 223(20)	(17:2) Heptadecynoic acid isomer	
40	57.9	309	97(100); 266(15); 292(10); 255(10); 141(5)	(20:1) Eicosenoic acid isomer	
41	59.3	333	289(100);	(14:0) Anacardic acid	
42	60.6	361	317(100); 299(20)	(16:0) Anacardic acid	1.124 ± 0.031[c]
43	60.9	331	287(100); 313(15)	(14:1) Anacardic acid	
44	61.5	337	97(100); 293(60); 183(40); 319(5)	(22:1) Erucic acid	1.351 ± 0.048[c,§]
45	61.5	289	245(100)	(19:4) Nonadecadiynoic acid isomer	1.351 ± 0.018[c,§]
46	61.9	315	271(100); 255(5);	(13:3) Anacardic acid	
47	63.1	317	273(100); 107(5);	(13:1) Anacardic acid	1.501 ± 0.015[c]
48	63.7	369	325(100);	(17:3) Anacardic acid	0.388 ± 0.007[c]
49	64.2	319	275(100);	(13:0) Anacardic acid	5.874 ± 0.273[c,#]
50	64.4	345	301(100);	(15:1) Anacardic acid	5.874 ± 0.273[c,#]
51	65.6	347	303(100)	(15:0) Anacardic acid	
52	65.8	373	329(100)	(17:1) Anacardic acid	

[a] quantified as gallic acid; [b]quantified as quercetin-3-*O*-glucoside; [c]quantified as (17:1)-anacardic acid. [*, ç, §, #] quantified together.

(Ferreira et al., 2022). Analogously, a resinous by product from Brazilian propolis exhibited a lower $O_2^{\bullet -}$ scavenging ability ($IC_{50} = 166.60$ μg/mL) than OPVS-E (de Francisco et al., 2018).

Regarding the ORAC assay, OPVS-E showed a poor quenching capacity towards ROO• (0.72 μmol TE/mg DW). However, a lower result (0.053 μmol TE/mg DW) was reported for *C. sativa* Mill. shell extract prepared by supercritical fluid extraction-CO_2 (Pinto et al., 2020).

3.8. Caco-2 and HT29-MTX cell viability

MTT assays were performed to evaluate the safety of the OPVS-E on two human intestinal cell lines, namely Caco-2 and HT29-MTX. These cell lines are widely used as physiologically relevant models of human intestinal epithelium, allowing for controlled *in vitro* experiments, reducing the need for animal testing, and providing valuable insights into bioactive compounds interaction with the intestinal environment before progressing to *in vivo* studies (Pinto, Silva, et al., 2021). As can be observed in Fig. 3, the exposure of both cell lines to increasing concentrations (62.5 – 1000 mg/L) of the OPVS-E led to an intestinal cell viability higher than 75 %. Specifically, the extract did not significantly ($p > 0.05$) affect the viability of the HT29-MTX cells, achieving results around 100 %. On the other hand, the exposure of Caco-2 cells to the highest tested concentration (1000 μg/mL) led to a significantly lower ($p < 0.05$) cell viability (75.93 %), due to an increased sensitivity of Caco-2 cells when compared to HT29-MTX, which was highlighted even by other authors (de Francisco et al., 2018; Pinto et al., 2019). Nevertheless, *Castanea sativa* Mill. shell extract obtained by SWE exhibited cell viabilities of 9.06 % and 6.29 %, respectively, for Caco-2 and HT29-MTX at the highest concentration tested (1000 μg/mL) (Pinto, Vieira, et al., 2021). Similarly, the resinous by-product from Brazilian propolis conducted to a significantly lower Caco-2 viability (<50 % at 1000 μg/mL) than OPVS-E (de Francisco et al., 2018).

Table 6
Inhibitory activity towards α–amylase and α –glucosidase and reactive oxygen species (ROS) scavenging capacity of OPVS-E. Results are reported as mean ± standard error ($n = 3$).

	Hypoglycaemic activity		Reactive oxygen scavenging capacity		
	α-Amylase IC_{50}, μg/mL	α–Glucosidase IC_{50}, μg/mL	$O_2^{\bullet -}$ IC_{50}, μg/mL	HClO IC_{50}, μg/mL	ROO• μmol TE/mg DW
OPVS-E	2.05 ± 0.84^{a}	41.07 ± 0.30^{b}	54.92 ± 2.36^{a}	4.70 ± 0.29^{a}	0.72 ± 0.07^{b}
Acarbose	8.93 ± 1.37^{a}	98.34 ± 1.78^{a}			
Gallic acid			10.39 ± 1.60^{c}	5.51 ± 0.34^{a}	7.51 ± 0.40^{b}
Catechin			26.24 ± 0.15^{b}	0.32 ± 0.02^{b}	237.11 ± 28.37^{a}

TE stands for Trolox equivalents. Different letters in the same column indicate significant differences (Tukey's test, $p < 0.05$).

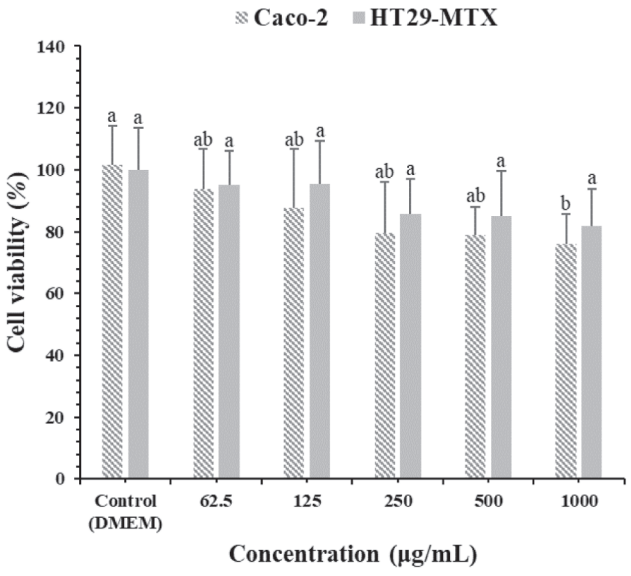

Fig. 3. Effects of OPVS-E on the viability of Caco-2 and HT29-MTX cell lines at a concentration range between 62.5 and 1000 μg/mL. The extract was assayed in quadruplicate and results are reported as mean ± SD of two independent experiments. Different letters (a, b) indicate significant differences (Tukey's test, $p < 0.05$) compared with control.

As far as we know, this is the first study that reports the impact of PVS on Caco-2 and HT29-MTX intestinal cell lines.

4. Conclusions

The application of the optimized MAE protocol determined by the RSM enabled a high recovery of antioxidants from *Pistacia vera* L. shells. Among the four independent variables investigated, the ethanol concentration was the one that affected the MAE of bioactive compounds from PVS. The experimental data confirmed the optimal MAE conditions estimated by the model (20 % EtOH, 1000 W, 135 s and 27.7 mL/g).

It is noteworthy that this method can be readily expanded for industrial use since ethanol is commonly utilized in the preparation of food supplements from natural extracts. Additionally, the industrial extraction of natural products using microwave irradiation has become a reality in industrial practices. HPLC/ESI-MS/MS analysis revealed the richness of the OPVS-E in gallic acid derivatives, hydrolysable tannins, flavonoids, fatty acids, and anacardic acids. Moreover, the OPVS-E exhibited a significant inhibitory activity towards α-amylase and α-glucosidase, which may be related to the high content of hydrolysable tannins and anacardic acids. Structure-activity relationships and multispectroscopic studies need to be further explored to better understand the individual compound contribution in such hypoglycaemic effect. No cytotoxic effects were observed on Caco-2 and HT29-MTX cells. Based on the results mentioned above, the OPVS-E can effectively constitute an option as novel anti-diabetic ingredient for the prevention and management of T2DM. Further *in vivo* and clinical studies are requested to fully validate this new application and to establish the anti-diabetic potential of the extract.

Funding

This work was financed by MUR ITALY PRIN 2022 PNRR (Project No. P2022MWY3P) and by national funds from FCT - Fundação para a Ciência e a Tecnologia, I.P., in the scope of the project UIDP/04378/2020 and UIDB/04378/2020 of the Research Unit on Applied Molecular Biosciences - UCIBIO and the project LA/P/0140/2020 of the Associate Laboratory Institute for Health and Bioeconomy - i4HB.

CRediT authorship contribution statement

Anna Elisabetta Maccarronello: Methodology, Validation, Formal analysis, Investigation, Writing – original draft. **Nunzio Cardullo:** Writing – review & editing, Visualization, Supervision, Methodology. **Ana Margarida Silva:** Investigation, Visualization. **Antonella Di Francesco:** Validation, Investigation. **Paulo C. Costa:** Writing – review & editing, Investigation. **Francisca Rodrigues:** Writing – review & editing, Visualization, Supervision, Resources, Investigation, Funding acquisition. **Vera Muccilli:** Writing – review & editing, Visualization, Supervision, Resources, Project administration, Funding acquisition, Conceptualization.

Declaration of competing interest

The authors declare that they have no known competing financial interests or personal relationships that could have appeared to influence the work reported in this paper.

Data availability

Data will be made available on request.

Acknowledgements

The authors gratefully acknowledge the Bio-Nanotech Research and Innovation Tower of the University of Catania (BRIT; project PONa3_00136) financed by the Italian Ministry for Education, University and Research MIUR, for making available the Synergy H1 microplate reader.

Anna Elisabetta Maccarronello is thankful for the PhD grant (D.M. n 1061, PON R&I 2014/2020, 2020/2021 – Cycle 37) financed by the Italian Ministry for Education, University and Research MIUR. Ana Margarida Silva is thankful for the Ph.D. grant (SFRH/BD/144994/2019) financed by POPH-QREN and subsidized by the European Science Foundation and Ministério da Ciência, Tecnologia e Ensino Superior. Francisca Rodrigues (CEECIND/01886/2020) is thankful for her contract financed by FCT/MCTES—CEEC Individual Program Contract.

Appendix A. Supplementary material

Supplementary data to this article can be found online at https://doi.org/10.1016/j.foodchem.2024.138504.

References

Alvi, T., Asif, Z., & Khan, M. K. I. (2022). Clean label extraction of bioactive compounds from food waste through microwave-assisted extraction technique-A review. *Food Bioscience, 46*. https://doi.org/10.1016/j.fbio.2022.101580

Bezerra, M. A., Santelli, R. E., Oliveira, E. P., Villar, L. S., & Escaleira, L. A. (2008). Response surface methodology (RSM) as a tool for optimization in analytical chemistry. *Talanta, 76*(5), 965–977. https://doi.org/10.1016/j.talanta.2008.05.019

Bonaccorso, A., Russo, G., Pappalardo, F., Carbone, C., Puglisi, G., Pignatello, R., & Musumeci, T. (2021). Quality by design tools reducing the gap from bench to bedside for nanomedicine. *European Journal of Pharmaceutics and Biopharmaceutics, 169*, 144–155. https://doi.org/10.1016/j.ejpb.2021.10.005

Cardullo, N., Floresta, G., Rescifina, A., Muccilli, V., & Tringali, C. (2021). Synthesis and in vitro evaluation of chlorogenic acid amides as potential hypoglycemic agents and their synergistic effect with acarbose. *Bioorganic Chemistry, 117*. https://doi.org/10.1016/j.bioorg.2021.105458

Cardullo, N., Leanza, M., Muccilli, V., & Tringali, C. (2021). Valorization of agri-food waste from pistachio hard shells: Extraction of polyphenols as natural antioxidants. *Resources-Basel, 10*(5). https://doi.org/10.3390/resources10050045

Cardullo, N., Muccilli, V., Cunsolo, V., & Tringali, C. (2020). Mass Spectrometry and H-1-NMR study of Schinopsis lorentzii (Quebracho) tannins as a source of hypoglycemic and antioxidant principles. *Molecules, 25*(14). https://doi.org/10.3390/molecules25143257

Cardullo, N., Muccilli, V., Pulvirenti, L., Cornu, A., Pouysegu, L., Deffieux, D., Quideau, S., & Tringali, C. (2020). *C*-glucosidic ellagitannins and galloylated glucoses as potential functional food ingredients with anti-diabetic properties: A study of α-glucosidase and α-amylase inhibition. *Food Chemistry, 313*. https://doi.org/10.1016/j.foodchem.2019.126099

Dahmoune, F., Boulekbache, L., Moussi, K., Aoun, O., Spigno, G., & Madani, K. (2013). Valorization of *Citrus limon* residues for the recovery of antioxidants: Evaluation and optimization of microwave and ultrasound application to solvent extraction. *Industrial Crops and Products, 50*, 77–87. https://doi.org/10.1016/j.indcrop.2013.07.013

Dahmoune, F., Nayak, B., Moussi, K., Remini, H., & Madani, K. (2015). Optimization of microwave-assisted extraction of polyphenols from *Myrtus communis* L. leaves. *Food Chemistry, 166*, 585–595. https://doi.org/10.1016/j.foodchem.2014.06.066

de Francisco, L., Pinto, D., Rosseto, H., Toledo, L., Santos, R., Tobaldini-Valério, Svidzinski, T., Bruschi, M., Sarmento, B., Oliveira, M.B.P.P., F., Rodrigues, F. (2018). Evaluation of radical scavenging activity, intestinal cell viability and antifungal activity of Brazilian propolis by-product. *Food Research International, 105*, 537-547. https://doi.org/10.1016/j.foodres.2017.11.046.

Erşan, S., Üstündağ, Ö. G., Carle, R., & Schweiggert, R. M. (2016). Identification of phenolic compounds in red and green pistachio (Pistacia vera L.) hulls (exo- and mesocarp) by HPLC-DAD-ESI-(HR)-MSn. *Journal of Agricultural and Food Chemistry, 64*(26), 5334–5344. https://doi.org/10.1021/acs.jafc.6b01745

FAOSTAT. Crops and livestock products (2021). Retrieved from: https://www.fao.org/faostat/en/#data/QCL Accessed 07/09/2023.

Ferreira, A. S., Silva, A. M., Pinto, D., Moreira, M. M., Ferraz, R., Švarc-Gajić, J., Costa, P. C., Delerue-Matos, C., & Rodrigues, F. (2022). New perspectives on the sustainable employment of chestnut shells as active ingredient against oral mucositis: A first screening. *International Journal of Molecular Sciences, 23*(23). https://doi.org/10.3390/ijms232314956

Fiorentino, T. V., Prioletta, A., Zuo, P., & Folli, F. (2013). Hyperglycemia-induced oxidative stress and its role in diabetes mellitus related cardiovascular diseases. *Current Pharmaceutical Design, 19*(32), 5695–5703. https://doi.org/10.2174/1381612811319320005

Gomes, A., Fernandes, E., Silva, A. M. S., Santos, C. M. M., Pinto, D., Cavaleiro, J. A. S., & Lima, J. L. F. C. (2007). 2-Styrylchromones: Novel strong scavengers of reactive oxygen and nitrogen species. *Bioorganic & Medicinal Chemistry, 15*(18), 6027–6036. https://doi.org/10.1016/j.bmc.2007.06.046

Hiew, C. W., Lee, L. J., Junus, S., Tan, Y. N., Chai, T. T., & Ee, K. Y. (2022). Optimization of microwave-assisted extraction and the effect of microencapsulation on mangosteen (Garcinia mangostana L.) rind extract. *Food Science and Technology, 42*. https://doi.org/10.1590/fst.35521

Jerz, G., Murillo-Velasquez, Skrjabin, I., Gök, R., & Winterhalter, P. (2012). Anacardic acid profiling in cashew nuts by direct coupling of preparative high-speed countercurrent chromatography and mass spectrometry (*prep*HSCCC-ESI-/APCI-MS/MS). *Recent Advances in the Analysis of Food and Flavors* (pp. 145-165) https://doi.org/10.1021/bk-2012-1098.ch011.

Kumar, R. V., & Sinha, V. R. (2012). Newer insights into the drug delivery approaches of α-glucosidase inhibitors. *Expert Opinion on Drug Delivery, 9*(4), 403–416. https://doi.org/10.1517/17425247.2012.663080

Lim, J., Ferruzzi, M. G., & Hamaker, B. R. (2022). Structural requirements of flavonoids for the selective inhibition of α-amylase versus α-glucosidase. *Food Chemistry, 370*. https://doi.org/10.1016/j.foodchem.2021.130981

Liu, X. C., Wang, Y. H., Zhang, J. C., Yang, L. L., Liu, S. Q., Taha, A. A., Wang, J., & Ma, C. (2020). Subcritical water extraction of phenolic antioxidants with improved α-amylase and α-glucosidase inhibitory activities from exocarps of *Castanea mollissima* Blume. *Journal of Supercritical Fluids, 158*. https://doi.org/10.1016/j.supflu.2019.104747

Lopez-Salazar, H., Camacho-Diaz, B. H., Ocampo, M. L. A., & Jimenez-Aparicio, A. R. (2023). Microwave-assisted extraction of functional compounds from plants: A review. *Bioresources, 18*(3), 6614–6638. https://doi.org/10.15376/biores.18.3.Lopez-Salazar.

Morais, S. M., Silva, K. A., Araujo, H., Vieira, I. G. P., Alves, D. R., Fontenelle, R. O. S., & Silva, A. M. S. (2017). Anacardic acid constituents from cashew nut shell liquid: NMR characterization and the effect of unsaturation on its biological activities. *Pharmaceuticals, 10*(1). https://doi.org/10.3390/ph10010031

Muccilli, V., Maccarronello, A. E., Rasoanandrasana, C., Cardullo, N., de Luna, M. S., Pittalà, M. G. G., Riccobene, P. M., Carroccio, S. C., & Scamporrino, A. A. (2023). Green^3: A green extraction of green additives for green plastics. *Heliyon*. https://doi.org/10.1016/j.heliyon.2024.e24469

Nayak, B., Dahmoune, F., Moussi, K., Remini, H., Dairi, S., Aoun, O., & Khodir, M. (2015). Comparison of microwave, ultrasound and accelerated-assisted solvent extraction for recovery of polyphenols from *Citrus sinensis* peels. *Food Chemistry, 187*, 507–516. https://doi.org/10.1016/j.foodchem.2015.04.081

Ngoh, Y. Y., & Gan, C. Y. (2016). Enzyme-assisted extraction and identification of antioxidative and alpha-amylase inhibitory peptides from Pinto beans (Phaseolus vulgaris cv. Pinto). *Food Chemistry, 190*, 331–337. https://doi.org/10.1016/j.foodchem.2015.05.120

Ou, B. X., Hampsch-Woodill, M., & Prior, R. L. (2001). Development and validation of an improved oxygen radical absorbance capacity assay using fluorescein as the fluorescent probe. *Journal of Agricultural and Food Chemistry, 49*(10), 4619–4626. https://doi.org/10.1021/jf010586o

Pandey, K. B., & Rizvi, S. I. (2009). Plant polyphenols as dietary antioxidants in human health and disease. *Oxidative Medicine and Cellular Longevity, 2*(5), 270–278. https://doi.org/10.4161/oxim.2.5.9498

Pinto, D., Cadiz-Gurrea, M. D., Sut, S., Ferreira, A. S., Leyva-Jimenez, F. J., Dall'Acqua, S., Segura-Carretero, A., Delerue-Matos, C., & Rodrigues, F. (2020). Valorisation of underexploited *Castanea sativa* shells bioactive compounds recovered by supercritical fluid extraction with CO_2: A response surface methodology approach. *Journal of CO_2 Utilization, 40*. https://doi.org/10.1016/j.jcou.2020.101194

Pinto, D., Franco, S. D., Silva, A. M., Cupara, S., Koskovac, M., Kojicic, K., Soares, S., Rodrigues, F., Sut, S., Dall'Acqua, S., & Oliveira, M. B. P. P. (2019). Chemical characterization and bioactive properties of a coffee-like beverage prepared from *Quercus cerris* kernels. *Food & Function, 10*(4), 2050-2060. https://doi.org/10.1039/c8fo02536c.

Pinto, D., Silva, A. M., Freitas, V., Vallverdú-Queralt, A., Delerue-Matos, C., & Rodrigues, F. (2021). Microwave-assisted extraction as a green technology approach to recover polyphenols from *Castanea sativa* shells. *Acs Food Science & Technology, 1*(2), 229–241. https://doi.org/10.1021/acsfoodscitech.0c00055

Pinto, D., Vieira, E. F., Peixoto, A. F., Freire, C., Freitas, V., Costa, P., Delerue-Matos, C., & Rodrigues, F. (2021). Optimizing the extraction of phenolic antioxidants from chestnut shells by subcritical water extraction using response surface methodology. *Food Chemistry, 334*. https://doi.org/10.1016/j.foodchem.2020.127521

Sanchez-Reinoso, Z., Mora-Adames, W. I., Fuenmayor, C. A., Darghan-Contreras, A. E., Gardana, C., & Gutierrez, L. F. (2020). Microwave-assisted extraction of phenolic compounds from *Sacha Inchi* shell: Optimization, physicochemical properties and evaluation of their antioxidant activity. *Chemical Engineering and Processing-Process Intensification, 153*. https://doi.org/10.1016/j.cep.2020.107922

Silva, A. M., Pinto, D., Moreira, M. M., Costa, P. C., Delerue-Matos, C., & Rodrigues, F. (2022). Valorization of kiwiberry leaves recovered by ultrasound-assisted extraction for skin application: A response surface methodology approach. *Antioxidants, 11*(4). https://doi.org/10.3390/antiox11040763

Sud, M., Fahy, E., Cotter, D., Brown, A., Dennis, E. A., Glass, C. K., Merrill, A. H., Murphy, R. C., Raetz, C. R. H., Russell, D. W., & Subramaniam, S. (2007). LMSD: LIPID MAPS structure database. *Nucleic Acids Research, 35*, D527–D532. https://doi.org/10.1093/nar/gkl838

Terzo, S., Baldassano, S., Caldara, G. F., Ferrantelli, V., Lo Dico, G., Mule, F., & Amato, A. (2019). Health benefits of pistachios consumption. *Natural Product Research, 33*(5), 715–726. https://doi.org/10.1080/14786419.2017.1408093

Toghiani, J., Fallah, N., Nasernejad, B., Mahboubi, A., Taherzadeh, M. J., & Afsham, N. (2023). Sustainable pistachio dehulling waste management and its valorization approaches: A review. *Current Pollution Reports, 9*(1), 60–72. https://doi.org/10.1007/s40726-022-00240-9

Toyomizu, M., Sugiyama, S., Jin, R. L., & Nakatsu, T. (1993). α-glucosidase and aldose reductase inhibitors: Constituents of cashew, anacardium-occidentale, nut shell liquids. *Phytotherapy Research, 7*(3), 252–254. https://doi.org/10.1002/ptr.2650070309

Tundis, R., Loizzo, M. R., & Menichini, F. (2010). Natural Products as α-amylase and α-glucosidase inhibitors and their hypoglycaemic potential in the treatment of diabetes: An update. *Mini-Reviews in Medicinal Chemistry, 10*(4), 315–331. https://doi.org/10.2174/138955710791331007

Ullah, A., Khan, A., & Khan, I. (2016). Diabetes mellitus and oxidative stress-A concise review. *Saudi Pharmaceutical Journal, 24*(5), 547–553. https://doi.org/10.1016/j.jsps.2015.03.013

Weremfo, A., Abassah-Oppong, S., Adulley, F., Dabie, K., & Seidu-Larry, S. (2023). Response surface methodology as a tool to optimize the extraction of bioactive

compounds from plant sources. *Journal of the Science of Food and Agriculture, 103*(1), 26–36. https://doi.org/10.1002/jsfa.12121

Yeganeh, M. M., Kaghazchi, T., & Soleimani, M. (2006). Effect of raw materials on properties of activated carbons. *Chemical Engineering & Technology, 29*(10), 1247–1251. https://doi.org/10.1002/ceat.200500298

Yuanu, B., Lu, M., Eskridge, K. M., & Hanna, M. A. (2018). Valorization of hazelnut shells into natural antioxidants by ultrasound-assisted extraction: Process optimization and phenolic composition identification. *Journal of Food Process Engineering, 41*(5). https://doi.org/10.1111/jfpe.12692